Seizure pathways changes at the subject-specific level via dynamic step effective network analysis

Jie Sun, Yan Niu, Yanqing Dong, Xubin Wu, Bin Wang, Mengni Zhou, Jie Xiang *, Jiuhong Ma *

***Abstract*—The variability in the propagation pathway in epilepsy is a main factor contributing to surgical treatment failure. Ways to accurately capture the brain propagation network and quantitatively assess its evolution remain poorly described. This work aims to develop a dynamic step effective network (dSTE) to obtain the propagation path network of multiple seizures in the same patient and explore the degree of dissimilarity. Multichannel stereo-electroencephalography (sEEG) signals were acquired with ictal processes involving continuous changes in information propagation. We utilized high-order dynamic brain networks to obtain propagation networks through different levels of linking steps. We proposed a dissimilarity index based on singular value decomposition to quantitatively compare seizure pathways. Simulated data were generated through The Virtual Brain, and the reliability of this method was verified through ablation experiments. By applying the proposed method to two datasets consisting of 29 patients total, the evolution processes of each patient's seizure networks was obtained, and the within-patient dissimilarities were quantitatively compared. Finally, three types of brain network connectivity patterns were found. Type I patients have a good prognosis, while type III patients are prone to postoperative recurrence. This method captures the evolution of seizure propagation networks and assesses their dissimilarity more reliably than existing methods, demonstrating good robustness for studying the propagation path differences for multiple seizures in epilepsy patients. The three different patterns will be important considerations when planning epilepsy surgery under sEEG guidance.**

***Index Terms*—Epilepsy; Propagation network; Dynamic step effective network; Dissimilarity**

Manuscript received October 09, 2023. This work was supported by the National Natural Science Functional of China (62376184 and 62176177), Shanxi Province Free Exploration Basic Research Project (YDZJSX20231A017) the National Natural Science Foundation of China (62303445), the China Postdoctoral Science Foundation (2023M733669), the Shanxi Province Application Basic Research Plan (20210302124550 and 202103021224384), the National Natural Science Foundation of Shanxi Province, grant number (20210302123112), Shenzhen Basic Research Project (Natural Science Foundation) (JCYJ20230807140719040) and Scientific Research Fund of Taiyuan University of Technology (2022QN036). (Corresponding authors: Jie Xiang; Jiuhong Ma)

Jie Sun, Yan Niu, Yanqing Dong, Xubin Wu and Bin Wang are with College of computer science and technology (College of Big Data), Taiyuan University of Technology, Taiyuan, China.

Mengni Zhou is with Shenzhen Institute of Advanced Technology, Chinese Academy of Sciences, Shenzhen, China.

Jie Xiang is with College of computer science and technology, Taiyuan University of Technology (College of Big Data), Taiyuan, China (Email: xiangjie@tyut.edu.cn).

Jiuhong Ma is with Neurosurgery Department, Shanxi Provincial People's Hospital, Taiyuan, China.(mjh2003@163.com).

I. Introduction

Focal epilepsy originates in a specific onset zone but may subsequently spread to neighboring regions of the brain until the entire cortex is potentially involved[1, 2]. An unresolved issue is how the seizures themselves vary among individual patients. Previous studies have found that seizures in individual patients have similar characteristics[3-6] and evolve through similar spatiotemporal neural dynamics sequences[7] or feature pathways[8]. However, there is also evidence that the various aspects of epilepsy can differ even in the same patient. Long-term electroencephalography (EEG) records in clinical practice indicate that a subset of patients have multiple types of epileptic seizure evolution[9-11]. It is possible that a given treatment may only target a subset of patients with seizures, resulting in the inability to control the complete range of seizures[12, 13]. Therefore, seizure variability is of great importance for the clinical management of these patients.

To design an optimal and comprehensive treatment plan, we need to understand the prevalence and characteristics of patient variability. Although some studies have conducted quantitative comparisons among patients with epileptic seizures[14-17], the current gold standard is still routine examination of the initial EEG by trained clinical doctors. This method is time-consuming and subjective, however, and may miss important functions, including network interactions that are difficult to detect visually. Therefore, we must use computational methods to objectively quantify the similarity of seizure pathways and design a reasonable surgical program.

Dynamic brain network connectivity reflects information interactions between brain regions, which can help reveal the evolution of seizure networks[18-20]. Nuttida Rungratsameetaweemana et al. applied a graph-theoretical approach to assess dynamic reconfigurations in functional brain connectivity before, during, and after seizures that displayed heterogeneous propagation patterns[21]. Brittany H. Scheid et al. calculated the average and modal controllability from each generated effective connectivity network to measure the time-varying controllability of the brain on an evolution graph of conditional network interaction[22]. Most existing studies focused on a single seizure and did not consider the effects of multiple seizures on patients[18, 21, 23-25]. Additionally, they used brain connectivity to evaluate the dynamic remodeling characteristics of epilepsy at different periods, including correlation, mutual information, and effective connectivity[26-28].

Because of the variety of approaches to constructing networks, most of them require the assumption of a specific model. However, transfer entropy (TE) does not need to be modeled in advance, so it has certain advantages, such as good correlation sensitivity and small detection errors[29]. However, to meet the requirements of clinical applications, further research is still needed, especially in capturing hierarchical propagation patterns in dynamic networks and developing robust systems that perform consistently given different patients.

One challenge in assessing the evolution of epileptic seizures is that brain connections have only first-order neighbor information. Because of the sequence in which nodes are propagated, the information propagation mode is of high order. Gabriel M. Schroeder et al. utilized sliding-window functional connectivity to study the dissimilarity of multiple seizures in the same patient, and they found variability in seizure network evolution[9]. Mariella Panagiotopoulou et al. tracked network dynamics and found that the evolution of multiple seizures in most subjects above chance level fluctuates on different timescales[30]. However, ways to accurately capture the brain communication network and quantitatively assess its evolution have not been well defined. The propagation path during an attack follows a certain order in terms of the nodes along which the attack propagates. Because effective networks cannot provide characteristic regions connected to brain regions at different link-step distance levels, the classical mathematical model cannot be directly applied. Dynamic networks are complex and contain a large amount of information; therefore, direct similarity comparisons will have time complexity, information redundancy and other problems.

In this study, we propose building a dynamic and effective network based on high-order information to capture the multilevel network of epilepsy propagation. As shown in Figure 1, we use three sets of subjects to construct a connectivity matrix under different time windows and then extract its high-order information step by step. The connection matrix obtained with this method in each time window then represents the propagation path mode at this time. A dissimilarity measurement method based on singular value decomposition is proposed to quantitatively compare each seizure in the same patient. The reliability of this method was verified by generating simulated data through The Virtual Brain (TVB). Our method quantifies and characterizes the within-patient variability in the evolution of the seizure network, finally yielding three types of epileptic seizure network connection patterns.

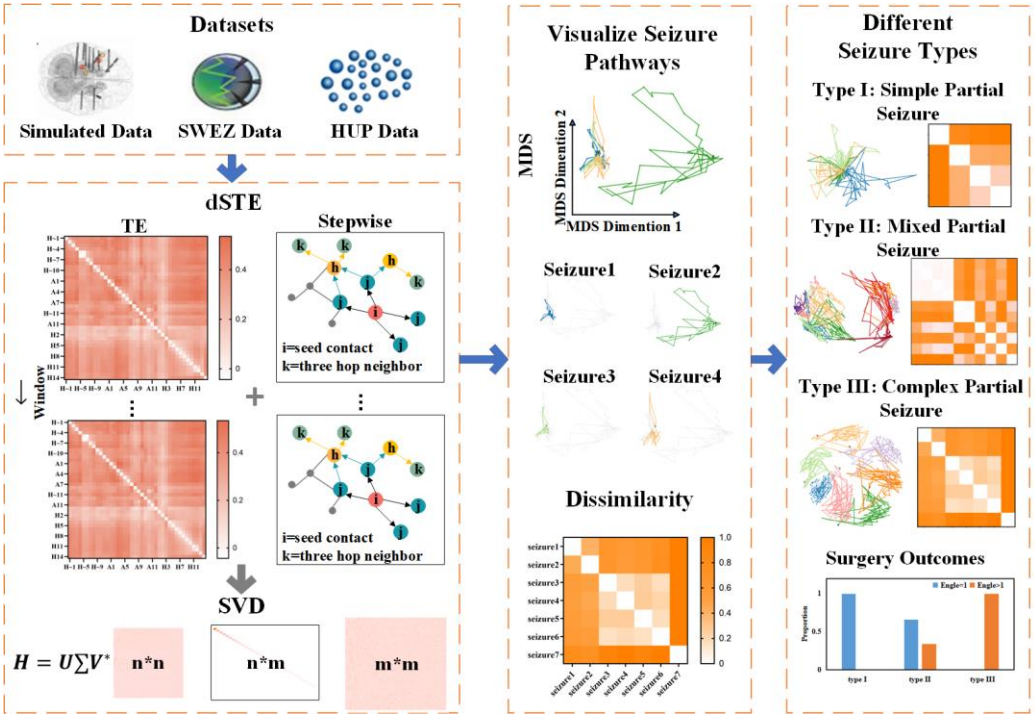

Fig. 1 Schematic illustration of the overall methodological approach. A: We first obtain the TE network, and then a three-step process is performed to capture the propagation of hierarchical information; B: the anatomical network is constructed from MRI and TI data, and by using the "Epileptor Model", the simulation data are finally obtained; C: the transmission path of a seizure in a clinical patient is obtained through the three steps.

II. METHODS

A. Study subjects

The data from two centers were used in this study: (1) the SWEZ dataset, consisting of 11 in the neurosurgery department of Shanxi Provincial People's Hospital; (2) the HUP dataset, a public dataset consisting of 18 patients from the Hospital of the University of Pennsylvania. To be included in the study, each patient was required to have had at least four seizures suitable for the analysis. and. The information collected from the stereo-electroencephalography (SEEG) data of the two datasets is shown in Appendix S1, Tables S1 and S2.

Preprocessing with the Brainstorm tool[31]: First, we removed bad channels, performed independent component analysis (ICA) to remove any artifacts, bandpass filtered the data at 0.16-97 Hz

and downsampled the frequency from 1000 Hz to 500 Hz. The bad channels are mainly determined by sEEG observation and doctor's record during operation. ICA-based artifact correction can separate and remove multiple artifacts from sEEG data through linear decomposition.

B. *Epileptor model*

In our study, simulated data were generated with the Epileptor model as the ground truth to verify dynamic step transfer entropy (dSTE). Figure 2 shows the default structural connectome of John Doe from the TVB and the subsequent use of the Epileptor model to simulate the iEEG data[32].

Mathematically, the Epileptor model is composed of five state variables coupled with two oscillating dynamical systems at three different time scales (see Appendix S2 for details). Proix et al. demonstrated that simple and complex seizure recruitment among brain regions can be modeled by coupling Epileptor nodes with permittivity-based coupling[33]. Hence, the Epileptor model is implemented here using the following eight equations adapted from the original five-equation model[32]:

$$\dot{x}_{1,i} = y_{1,i} - f_1(x_{1,i}, x_{2,i}) - z + I_1 \quad (1)$$

$$\dot{y}_{1,i} = 1 - 5x_{1,i}^2 - y_{1,i} \quad (2)$$

$$\dot{z}_i = \frac{1}{\tau_0}\left(4(x_{1,i} - x_0) - z_i - \sum_{j=1}^{N} KC_{ij}\,(x_{1,j} - x_{1,i})\right) \quad (3)$$

$$\dot{x}_{2,i} = -y_{2,i} + x_{2,i} - x_{2,i}^3 + I_2 + 0.002g(x_{1,i}) - 0.3(z_i - 3.5) \quad (4)$$

$$\dot{y}_{2,i} = \frac{1}{\tau_2}(-y_{2,i} + f_2(x_{2,i})) \quad (5)$$

where

$$f_1(x_{1,i}, x_{2,i}) = \begin{cases} x_{1,i}^3 - 3x_{1,i}^2 & if\, x_{1,i} < 0 \\ (x_{2,i} - 0.6(z_i - 4)^2)x_{1,i} & if\, x_{1,i} \geq 0 \end{cases} \quad (6)$$

$$f_2(x_{2,i}) = \begin{cases} 0 & if\, x_{2,i} < -0.25 \\ 6(x_{2,i} + 0.25) & if\, x_{2,i} \geq -0.25 \end{cases} \quad (7)$$

$$g(x_{1,i}) = \int_{-t_0}^{t} exp^{-\gamma(t-\tau)}\, x_{1,i}(\tau)dt \quad (8)$$

where τ_0 = 2857, τ_2= 10, I_1 = 3.1, I_2 = 0.45, and γ = 0.01. The parameter x0 indicates the excitability of the brain region. When $x_0 > -2.1$. For the simulation data, $x_0 = -1.5$ represents the epileptic zone (EZ), early propagation nodes are represented by $x_0 = -1.8$, and $x_0 = -2.0$ represents late propagation nodes. In all other regions, x_0 is set to −3.0. Simulated SEEG data are generated by projecting the local field potential given by x_1 (t) + x_2 (t) into the sensor space through a linear transformation. Simulations are performed in TVB using the Heun integration scheme with a time step size of 0.05 ms for 10000 ms.

Specifically, for seizure 1, the x_0 values of the EZ regions are set to -3.0. The $x_0$values of the early propagation regions are set to -1.8. The x_0 values of the late propagation region are set to −2.0. Similar values are set for the other seizures; the specific locations can be seen in Table 1. The propagation paths designed for seizures 1 and 2 are similar, as are those designed for seizures 4 and 5.

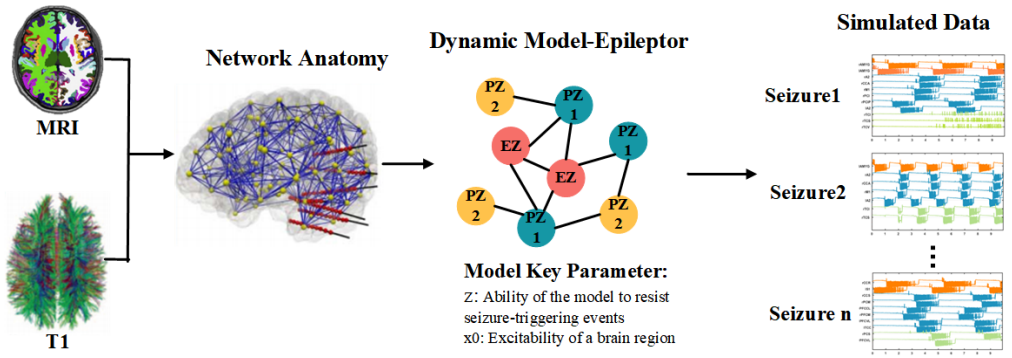

Fig. 2 Simulated data generation: with the default structural connectome of John Doe, we used the Epileptor model to simulate the sEEG data.

TABLE 1 Specific simulation locations

	x_0=-3.0	x_0=-1.8	x_0=−2.0
Seizure 1	rAMYG, lAMYG	rA2, rCCA, rM1, rPCI, rPCIP, and lA2	rTCI, rTCS and rTCV
Seizure 2	rPHC, rHC	rAMYG, rTCI, rTCS, lHC and lPHC	rA2, rCCA and rTCV
Seizure 3	lAMYG	rA2, rCCA, rM1 and lA2	rTCI and rTCS
Seizure 4	rCCR, rCCS	rPCM, rPCS, rPFCCL, rPFCM and rPFCPOL	lPCI, lPFCPOL and lPFCVL
Seizure 5	rCCR, lS1	rCCS, rPCM, rPFCCL, rPFCM and lPFCVL	lTCC, rPCS and rPFCVL

C. *Dynamic step transfer entropy*

In this section, we propose dSTE to objectively explore epileptic seizure variability. First, we partition each seizure with a 1-s sliding window. Then, we use the step effective connection capture propagation network. Finally, the obtained matrices are combined according to the time window order to obtain matrix *H* (Figure 3).

Kaiser and Schreiber proposed transfer entropy as an estimation of the information flow from one time series to another[34]. Compared with other model-based methods, TE has certain advantages in terms of correlation sensitivity[35, 36]. Therefore, TE was ultimately selected to build an effective network between different regions[37]. A brief overview of TE is given below.

Given system X and system Y, $\{x_i\}_{i=1}^N$ and $\{y\}_{i=1}^N$ denote the corresponding time series. The degree of information flow propagation between variables is obtained by calculating information entropy, which is defined as follows:

$$H_X = -\sum_i P(x_i)\log P(x_i) \quad (9)$$

Schreiber proposed TE to detect asymmetry in system interactions. We assume that the system under study is a stationary Markov process of order k, so each observation xi can be regarded as a state of Markov process and satisfies:

$$p(x_{i+1}|x_i,\dots,x_{i-k+1}) = p(x_{i+1}|x_i,\dots,x_{i-k}) \quad (10)$$

Taking full advantage of all previous states, the average amount of information transmitted for the most recent observation x_{i+1} is as follows:

$$h_x = -\sum_i p(x_{i+1}|x_i,\dots,x_{i-k+1})\log p(x_{i+1}|x_i,\dots,x_{i-k+1}) \quad (11)$$

Given the connection between the two systems X and Y, if there is no information flow between X and Y, then $p(x_{i+1}|x_i,\dots,x_{i-k+1}) = p(x_{i+1}|x_i,\dots,x_{i-k+1},y_i,\dots,y_{i-l+1})$. Therefore, the effect to which a system X is affected by system Y is measured by calculating the difference between two probabilities, $p(x_{i+1}|x_i,\dots,x_{i-k+1})$ and $p(x_{i+1}|x_i,\dots,x_{i-k+1},y_i,\dots,y_{i-l+1})$. Based on the Kullback entropy, which is a pleasant method based on the concept of backoff entropy and h_x to measure the difference in distribution, the transfer entropy is given by Schreiber as follows:

$$TE(Y \to X) = \sum_{x_{i+1},x_i^{(k)},y_i^{(l)}} p\left(x_{i+1},x_i^{(k)},y_i^{(l)}\right) log \frac{p\left(x_{i+1}|x_i^{(k)},y_i^{(l)}\right)}{p\left(x_{i+1}|x_i^{(k)}\right)} \quad (12)$$

$$x_i^k = p(x_{i+1}|x_i,\dots,x_{i-k+1}) \quad (13)$$

$$y_i^l = p(x_{i+1}|x_i,\dots,x_{i-k+1},y_i,\dots,y_{i-l+1}) \quad (14)$$

The transfer entropy from Y to X is essentially the information that Y changes with the uncertainty of X, that is, the size of the amount of information that Y transfers to X, quantifying the degree of statistical dependence derived from Y but not those originating from a common history, which is better than the standard mutual information of standard time delay.

As an input to the STE analysis, we first computed the individual TE matrices. We obtained an N-by-N matrix, where N is the sum of the contacts on all electrodes. Then, a Fisher transformation was applied to the resulting effective matrix. Next, we applied an FDR (Benjamini and Hochberg) correction at the 0.001 level to control for the rate of false positives in the final network adjacency matrices. Finally, we binarized the resulting FDR thresholded matrices to obtain directed graphs for each individual that will serve as input data for the STE analysis.

In our framework, a step refers to the number of links (edges) that belong to a path connecting a node to the target area. The high-order network is solved by the following formula:

$$STE^K = STE^1 * STE^{K-1}, \quad k \geq 2 \quad (15)$$

Specifically, step 1 is the initial TE matrix, which can capture the direct neighbors of the seed node. Step 2 captures two-hop neighbors, and step 3 captures three-hop neighbors. Through experimental studies and clinical observation, a relatively complete multimodal integration network can be captured in step 3. Therefore, we used the third-order network to extract the seizure brain network.

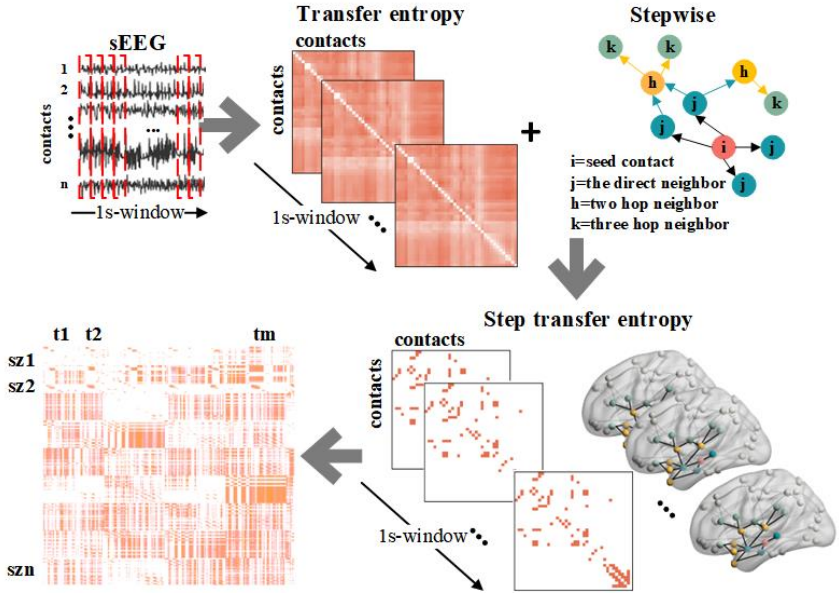

Fig. 3 Step dynamic transfer entropy analysis: First, we divide each episode with a 1-s sliding window. Then, we use transfer entropy combined with step 3 to obtain an effectively connected capture propagation network. Finally, matrix H is obtained by combining the obtained matrices in the order of the time window.

D. MDS index

Because of the high dimensionality of this network space, it

is not feasible to directly observe the seizure pathways. However, they can be approximated in two dimensions (2D). MDS was used to project all seizure time windows into 2D space, allowing seizure pathway visualization through network space. Each point corresponds to a seizure time window that is more similar to the network time window, and the dynamic position is closer in the projection. In the same seizure, continuous time windows are connected to visualize the seizure pathways.

The basic idea of multidimensional scaling (MDS) is to ensure that the relative distance between samples remains unchanged after the high-order space is mapped to the low-dimensional space. The algorithm is as follows:

Step 1: Calculate the distance among sample points in the original space. Taking Euclidean distance as an example, MDS should project the original d-dimensional space to a lower-dimensional space Z while maintaining the distance among sample points unchanged before and after dimension reduction. The formula is as follows:

$$d_{ij}^2 = ||Z_i - Z_j||^2 \tag{16}$$

Step 2: Calculate the inner product matrix B.

$$\sum_i Z_i = 0 \tag{17}$$

$$\sum_{i=1}^N d_{ij}^2 = \sum_{i=1}^N ||Z_i||^2 + N||Z_j||^2 \tag{18}$$

$$\sum_{j=1}^N d_{ij}^2 = \sum_{j=1}^N ||Z_j||^2 + N||Z_i||^2 \tag{19}$$

$$\sum_{i=1}^N \sum_{j=1}^N d_{ij}^2 = \sum_{i=1}^N \sum_{j=1}^N ||Z_j||^2 + N||Z_i||^2 = 2N \sum_{i=1}^N d_{ij}^2 \tag{20}$$

Define inner product matrix B, $B = Z^T Z$. Using the above formula, the element values in matrix B can be derived as follows:

$$b_{ij} = -0.5\left(\frac{1}{N^2}\sum_{i=1}^N \sum_{j=1}^N d_{ij}^2 - \frac{1}{N}\sum_{i=1}^N d_{ij}^2 - \frac{1}{N}\sum_{j=1}^N d_{ij}^2 + d_{ij}^2\right) \tag{21}$$

Step 3: Eigenvalue decomposition is performed on matrix B to obtain the eigenvalue matrix and eigenvector matrix:

$$B = V \wedge V^T \tag{22}$$

Step 4: The first z-term of the largest eigenvalue matrix and its corresponding eigenvector are taken to form the reduced dimension Z-matrix:

$$Z = V \wedge^{1/2} \tag{23}$$

The MDS algorithm only relies on the distance matrix of the sample, and the method does not need any other prior knowledge. After dimension reduction, the relative relationships among the samples in the original space are maintained, producing a better visualization effect.

E. Dissimilarity based on singular value decomposition

The matrix H contains noise, data redundancy and high complexity. We use singular value decomposition (SVD) to extract the key information in the matrix for quantitative analysis.

$$H = U\sum V^* \tag{24}$$

where U is an N * N left matrix; $\sum$ is a positive semidefinite N*M diagonal matrix; and V^*, the conjugate transpose of V, is an M*M right matrix. $\sum$ Diagonal elements $\sum_I$ are the singular values of H, representing r important features in the original matrix.

On the basis of the singular value matrix, we compared the dissimilarity matrix D of multiple seizures in each patient. A low dissimilarity indicates that the two seizures have similar pathways through network space.

$$D(i,j) = |\sum n_{ij} - \sum m_{ij}| \tag{25}$$

where $\sum n$ for the first seizure, and $\sum m$ for the other seizure.

III. RESULTS

A. Simulation data verify the reliability of dSTE

In this paper, we generated five seizures from simulated data using the Epileptor model in TVB to verify the accuracy of our method. We used ablation experiments to verify the reliability of dSTE. The ability of TE, STE and dSTE to capture multiple seizure propagation networks is shown in Figure 4. By simulating five seizures, sEEG data showed that the first and second seizures were similar, the fourth and fifth seizures were similar, and the electrodes involved in the third seizure were between those of the second and fourth seizures. The specific locations are shown in Table S3. TE yielded three seizure propagation patterns, but there was a deviation in the relative position of the third seizure. STE has higher-order information, and although three types of seizure propagation pattern were obtained and the relative positions of each seizure were basically correct, the pattern of path changes cannot be seen. After adding time information to the dSTE, more accurate results are obtained.

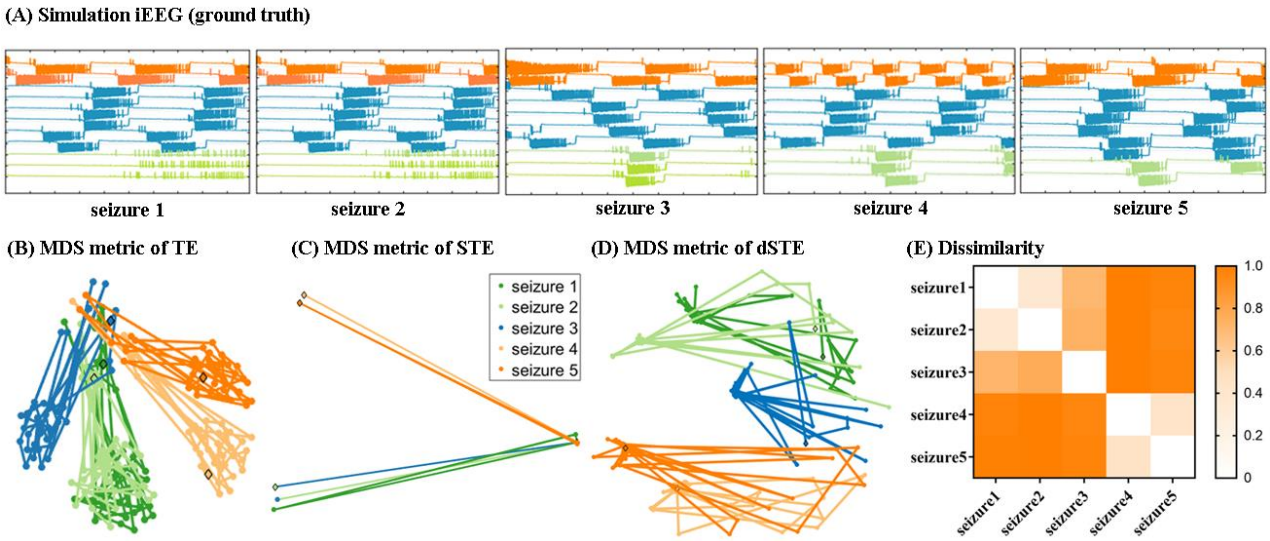

Fig. 4 Using simulated data for ablation experiments to verify the superiority of dSTE: (A) simulated iEEG data for known seizure types; (B) path pattern of multiple seizures obtained by TE; (C) path pattern of multiple seizures obtained by STE; (D) path pattern of multiple seizures obtained by dSTE; (E) dissimilarity matrix for the simulated data.

B. Visualizing and quantifying within-patient variability

Our first goal is to objectively compare the evolution of epileptic seizure networks in patients. For each patient, we calculated the effective connectivity in the sliding window. Therefore, the interaction between sEEG channels can be described by a high-order connection matrix in each time window that represents the evolution of the network dynamics of the epileptic seizure propagation path mode. By converting seizures in this way, we formulate seizure comparison as a comparison of seizure pathways (or trajectories) through high-dimensional network space. The MDS network space provides an intuitive visual comparison of epileptic seizure pathways within the same patient.

We identified three types of patients based on the seizure network dissimilarity (Figures 5, 6, and 7). Type I patients have high consistency in each seizure pathway and high similarity in the propagation path involved and are called simple patients. Type II patients are called mixed type patients; although they present with many types of seizures, they all obey certain rules, and there are certain similarities within multiple seizures. In type III patients, there is a large degree of dissimilarity directly among all seizure pathways, and so they are also called complex patients.

An example type I patient, patient ID06, is illustrated in Figure 5. The projections demonstrate that two seizures seem to follow approximately the same pathway (seizures 3 and 4). The dissimilarity matrix of all patients' seizures quantifies the difference in network evolution for each pair of seizures: low dissimilarity indicates that the two seizures have similar pathways. The pathways change as the number of seizures increases. However, in aggregate, the seizure pathways tend to be similar overall.

The results for a typical type II patient, patient ID05, are illustrated in Figure 6. The projections suggest that four seizures follow approximately the same pathway (seizures 1, 2, 3 and 4), four follow part of the same pathway (seizures 5, 6, 8 and 10), and two follow completely distinct pathways (seizures 7 and 9) through the network space. We can also clearly see these three propagation modes in the heatmap.

An example type III patient, patient ID10, has their results illustrated in Figure 7. We find that the overall presentation of the patient's multiple seizures is chaotic and that the similarity among them is low. Assessment of the dissimilarity shows that three seizures may follow approximately the same pathway (seizures 2, 3 and 5).

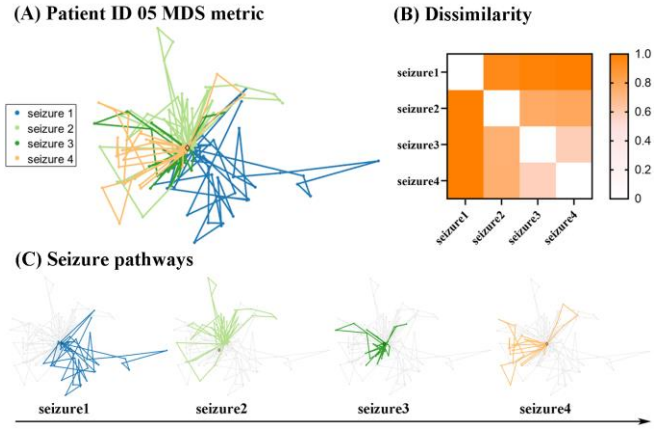

Fig. 5 Visualizing and comparing seizure pathways through network space in an example type I patient, patient ID05. (A) MDS projects all seizure time windows into 2D space. (B) The dissimilarity matrix of all the patient's seizures quantifies the difference in the network evolution of each pair of seizures. (C) Pathway evolution of epileptic seizures in the patient.

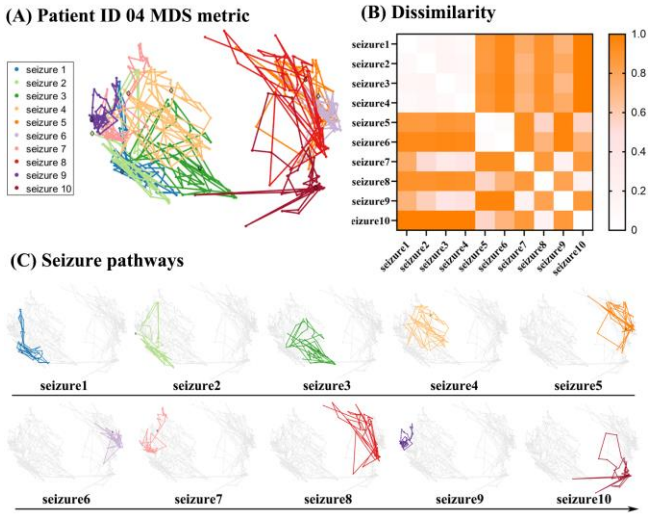

Fig. 6 Visualizing and comparing seizure pathways through network space in an example type II patient, patient ID04. (A) MDS projects all seizure time windows into 2D space. (B) The dissimilarity matrix of all the patient's seizures quantifies the difference in network evolution of each pair of seizures. (C) Pathway evolution of epileptic seizures in the patient.

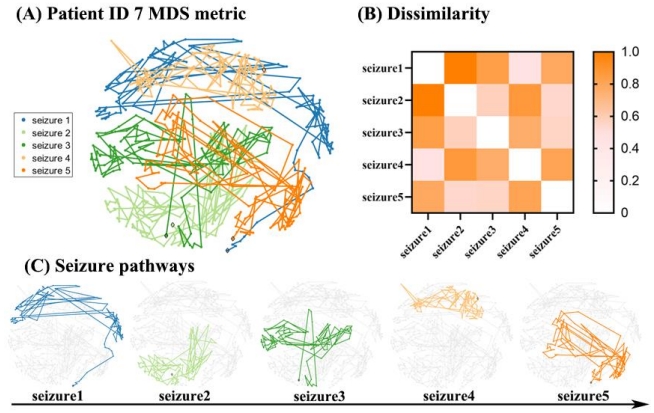

Fig. 7 Visualizing and comparing seizure pathways through network space in an example type III patient, patient ID7. (A) MDS projects all seizure time windows into 2D space. (B) The dissimilarity matrix of all the patient's seizures quantifies the difference in network evolution of each pair of seizures. (C) Pathway evolution of epileptic seizures in the patient.

C. Surgical outcomes for the three types of patients

In this study, we obtained the seizure types for 29 subjects, as shown in Figure 8(A). The Engel grades for the three types of patients were compared, as shown in Figure 8(B). We observed that type I patients had a better surgical outcome (Engle grade 1). Type III patients had a poor surgical outcome and a high risk of postoperative recurrence, which is consistent with our hypothesis: the lower the dissimilarity of patients with multiple seizures, the easier it is to locate the surgical resection area. Even if a few seizures are less frequently observed, there will be little impact on the surgical results. However, for patients with large dissimilarity among their seizures, if the situation for each seizure is not evaluated, it is likely to lead to surgical failure.

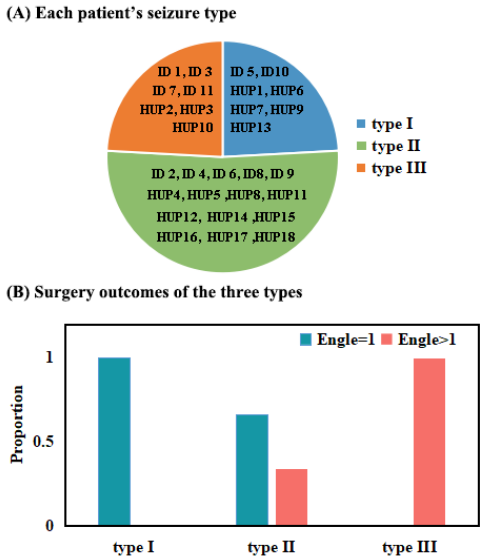

Fig. 8 Type of seizure in all subjects and its association with surgery outcome: Type I is simple patients for whom postoperative results were good. Type II is mixed patients. Type III patients are complex patients whose postoperative results are poor.

IV. Discussion

We proposed dSTE, which captured the propagation network of multiple seizures in the same patient. Since the seizure process is dynamic, the existing effective network framework cannot capture the high-order propagation mode in the dynamic network space. High-order dynamic brain networks can be used to obtain the propagation network through different levels of connection steps. Due to the high complexity and information redundancy of the constructed brain network, we proposed a dissimilarity index based on SVD to quantitatively assess the differences between multiple seizures.

Some studies have begun to focus on whether there are differences in the evolution of the networks of multiple seizures in the same epilepsy patient[30, 38, 39]. Ma et al. used the multiple seizure data from the same patient to calculate a synchronization index based on phase space reconstruction and mutual information to build a dynamic functional network model of seizures. The results showed that this model described the functional cooperation between various brain regions and the state transition in the seizure process[40]. Panagiotopoulou et al. quantified the duration of seizures using patient sEEG data over long periods (2-12 days). By using multiple seizures, it was found that the sEEG signal fluctuates in different frequency bands on different time scales, and this variability follows a specific pattern[30]. Schroeder et al. analyzed the iEEG data of patients with multiple seizures, quantitatively compared the evolution of patients' seizure networks, and found that the variability in the epileptic seizure paths can be reflected through the network dynamic space; that is, there are certain differences between multiple seizures of the same patient, but this difference cannot be better reflected through topological attributes such as the characteristic path of the network space[38]. Therefore, existing studies have only revealed changes in

network topology attributes when seizures spread, and no studies have revealed the dynamic evolution of seizure propagation paths when multiple, different seizures occur in the same patient. This is mainly because existing brain network analysis technologies cannot extract effective networks with propagation path information.

Through stepwise and time windows, our study successfully captured the higher-order networks that represent the propagation path of epilepsy. The reliability of the method was verified by using simulated data, as shown in Figure 4. The relative position of the third seizure obtained by TE is biased, mainly due to the lack of higher-order information in the TE method, which cannot successfully capture the propagation path. The STE method cannot discern the pattern of path changes because it only considers third-order matrices and ignores many temporal characteristics. The dSTE technique can capture both accurate propagation paths and temporal information, thus successfully capturing the variability in the networks of multiple seizures, proving the necessity of high-order information and dynamism. Previous studies have mainly applied dynamic functional connectivity in constructing high-order networks and assessed differences among multiple seizures through dimensionality reduction visualization[8, 30]. Our study constructed a dynamic high-order effective network that can capture directional information and reliable propagation paths between electrodes. We further conducted comparative experiments in this study, as shown in Table 2. Among the 29 subjects shown, 22 subjects maintained a high degree of consistency with previous studies, while the results of others were inconsistent. Patients with higher consistency also had better outcomes, lower Engle grades, and relatively simple modes of propagation. The prognosis of patients with inconsistencies is poor, and the difference among multiple seizures is greater. For these inconsistent subjects, we analyzed the pattern of change in the sEEG data. As shown in Figure 9, we can clearly see that the patient's first, third, and fourth seizures are more consistent, and the second seizure involves a wider range of contacts, which is consistent with the findings of this study. In summary, our study is closer to the truth on the basis of the existing research.

In this study, three types of seizure pattern were obtained, and their corresponding surgical results were consistent with clinical knowledge. The propagation network of type I patients with multiple seizures is relatively concentrated, which means that only one focal seizure network is involved, and the clinical manifestation is half retention of consciousness. This type of patient likely has better results after undergoing surgical resection. Type II patients demonstrate multiple types of propagation networks, and we speculate that their seizures propagate from the region of origin to the nearby brain network. If comprehensive postoperative results are considered during surgical resection, incomplete consideration will lead to recurrence. The propagation network involved in type III patients is relatively complex, and there is significant inconsistency among multiple seizures. We speculate that they are tonic-clonic seizures, greatly affecting the patient's cognition. The seizures may be transmitted directly from the region of origin to the insular region, with a faster rate of propagation to the entire brain than in the other patterns. This also leads to poor surgical outcomes for this type of patient, as shown in Figure 8.

There are some limitations in our study. Due to the short preoperative monitoring time and limited spatial coverage of the recording electrodes, some potential seizure pathways may not have been captured. It is evident that acknowledgement of the variation in the propagation pattern of epilepsy has increased the complexity and difficulty of surgical planning. Based on the results of our study, computer tools can be used to quickly and accurately determine the type of epileptic seizure. Future research should be conducted that fully considers the differences among multiple seizures in the patients, predict propagation pathways, and identify the "critical nodes" that contribute the most to the generalization of seizures to customize personalized surgical plans. We will conduct further research to find the optimal target for clinical intervention.

TABLE 2 Comparison results with the previous study

	Number of subjects	Engle	Possible reason
Consistent	22	1, 2	The patient propagation mode is relatively simple, and the postoperative outcome is good, so it is easy to distinguish multiple seizures.
Inconsistent	7	3, 4	The mode of patient propagation is complex, and the postoperative outcome is poor, so it is difficult to distinguish multiple seizures

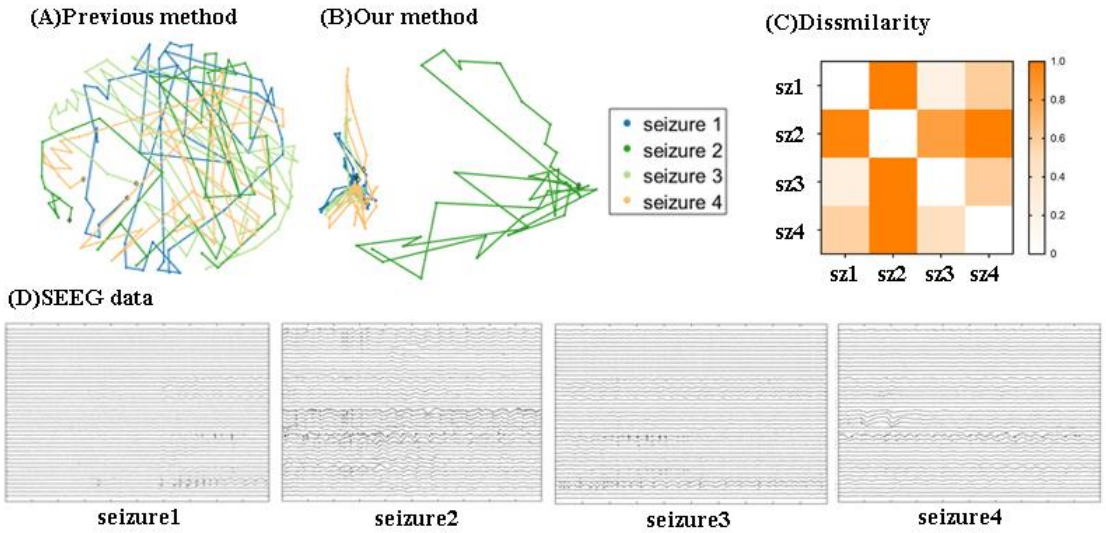

Figure 9 ID02 comparison results.

V. Conclusion

In conclusion, the proposed dSTE method showed satisfactory results in capturing the propagation networks of multiple seizures in the same patient, and it has a significant advantage in exploring high-order propagation patterns in dynamic network spaces. The dissimilarity index based on SVD can accurately assess differences among multiple seizures. The method is characterized by low time complexity and good robustness and should be widely applied in clinical practice. When planning epilepsy surgery under sEEG guidance, the three different propagation modes identified in this study will be important considerations.

References

[1] ROSENOW, F. Presurgical evaluation of epilepsy [J]. Brain, 2001, 124(9): 1683-700.
[2] ABBOUD M A, KAMEN J L, BASS J S, et al. Actigraphic correlates of neuropsychiatric symptoms in adults with focal epilepsy [J]. Epilepsia, 2023, 64(6): 1640-52.
[3] SCHINDLER K, GAST H, STIEGLITZ L, et al. Forbidden ordinal patterns of periictal intracranial EEG indicate deterministic dynamics in human epileptic seizures [J]. Epilepsia, 2011, 52(10): 1771-80.
[4] ESKANDAR E N, BROWN E N, HALGREN E, et al. Single-neuron dynamics in human focal epilepsy [J]. 2011.
[5] CATHERINE, SCHEVON, SHENNAN, et al. Evidence of an inhibitory restraint of seizure activity in humans [J]. Nature Communications, 2012.
[6] GREENBERG A, DICKSON C T. Spontaneous and electrically modulated spatiotemporal dynamics of the neocortical slow oscillation and associated local fast activity [J]. Neuroimage, 2013, 83(Complete): 782-94.
[7] BURNS S P, SANTANIELLO S, YAFFE R B, et al. Network dynamics of the brain and influence of the epileptic seizure onset zone [J]. Proceedings of the National Academy of Sciences of the United States of America, 2014, 111(49): E5321.
[8] SCHROEDER G M, DIEHL B, CHOWDHURY F A, et al. Seizure pathways change on circadian and slower timescales in individual patients with focal epilepsy [J]. Proceedings of the National Academy of Sciences of the United States of America, 2020, 117(20): 11048-58.
[9] SCHROEDER G M, CHOWDHURY F A, COOK M J, et al. Seizure pathways and seizure durations can vary independently within individual patients with focal epilepsy [J]. 2021.
[10] KING-STEPHENS D, MIRRO E, WEBER P B, et al. Lateralization of mesial temporal lobe epilepsy with chronic ambulatory electrocorticography [J]. Epilepsia: Journal of the International League against Epilepsy, 2015, 6.
[11] FREESTONE, DEAN, R., et al. Human focal seizures are characterized by populations of fixed duration and interval [J]. Epilepsia Journal of the International League Against Epilepsy, 2016.
[12] EWELL L A, LIANG L, ARMSTRONG C, et al. Brain State Is a Major Factor in Preseizure Hippocampal Network Activity and Influences Success of Seizure Intervention [J]. Journal of Neuroscience the Official Journal of the Society for Neuroscience, 2015, 35(47): 15635-48.
[13] WENDLING F, BELLANGER J J, BADIER J M, et al. Extraction of spatio-temporal signatures from depth EEG seizure signals based on objective matching in warped vectorial observations [J]. IEEE Transactions on Biomedical Engineering, 1996, 43(10): p.990-1000.
[14] DORR V L, CAPAROS M, WENDLING F, et al. Extraction of reproducible seizure patterns based on EEG scalp correlations [J]. Biomedical Signal Processing & Control, 2007, 2(3): 154-62.
[15] NEMETH M. Segmentation and Classification of Zn-Al-Mg-Sn SEM BSE Microstructure [J]. Applied Sciences, 2023, 13.
[16] BOUQUIN-JEANNèS R L, WENDLING F, FAUCON G, et al. Mise en correspondance de relations inter-structures lors de crises d'épilepsie [J]. IRBM, 2002, 23(1): 4-13.
[17] FRANASZCZUK P J, BERGEY G K, DURKA P J. Time-frequency analysis of mesial temporal lobe seizures using the matching pursuit algorithm; proceedings of the Society for Neuroscience Abstracts, F, 1996 [C].
[18] SIMULA S, GARNIER E, CONTENTO M, et al. Changes in local and network brain activity after stereotactic thermocoagulation in patients with drug‐resistant epilepsy [J]. Epilepsia, 2023, 64,1582 - 93.
[19] HASHEMI M, VATTIKONDA A N, JHA J, et al. Amortized Bayesian inference on generative dynamical network models of epilepsy using deep neural density estimators [J]. Neural Networks: The Official Journal of the International Neural Network Society, 2023.
[20] XI Z, SONG C, ZHENG J, et al. Brain Functional Networks with Dynamic Hypergraph Manifold Regularization for Classification of End-Stage Renal Disease Associated with Mild Cognitive Impairment [J]. 2023, 6): 24.
[21] RUNGRATSAMEETAWEEMANA N, LAINSCSEK C, CASH S S, et al. Brain network dynamics codify heterogeneity in seizure propagation [J]. Cold Spring Harbor Laboratory, 2021.
[22] SCHEID B H, ASHOURVAN A, STISO J, et al. Time-evolving controllability of effective connectivity networks during seizure progression [J]. 2020.
[23] DANIELE B, HALIMA A, DISHA S, et al. Identifying brain network dysfunctions during epileptogenesis in a model of temporal lobe epilepsy [J]. Frontiers in Neuroscience, 2015, 9.
[24] ZHANG G, ZHU Q, YANG J, et al. Functional Brain Connectivity Hyper-Network Embedded with Structural Information for Epilepsy Diagnosis [J]. International Journal of Image and Graphics, 2022, 22(04).

[25] SCHEID B H, ASHOURVAN A, STISO J, et al. Time-evolving controllability of effective connectivity networks during seizure progression [M]. 2020.
[26] BLUMENFELD, H. Positive and negative network correlations in temporal lobe epilepsy [J]. Cerebral Cortex, 2004, 14(8): 892-902.
[27] RAJAGURU H, PRABHAKAR S K. Insight to mutual information and matrix factorization with linear neural networks for epilepsy classification from EEG signals [J]. 2019.
[28] RUSSO S, MIKULAN E, ZAULI F M, et al. Neocortical and medial temporal seizures have distinct impacts on brain responsiveness [J]. Epilepsia, 2023, 64(6): e118-e26.
[29] NAKAJIMA K, SCHMIDT N, FEIFER R P. Measuring information transfer in a soft robotic arm [J]. Bioinspiration & Biomimetics, 2015, 10(3):
[30] PANAGIOTOPOULOU M, PAPASAVVAS C A, SCHROEDER G M, et al. Fluctuations in EEG band power at subject-specific timescales over minutes to days explain changes in seizure evolutions [J]. Human brain mapping, 2022, 43(8): 2460-77.
[31] STROHMANN T, SIEMON D, ROBRA-BISSANTZ S. brAInstorm: Intelligent Assistance in Group Idea Generation; proceedings of the 12th International Conference on Design Science Research in Information Systems and Technology (DESRIST), Karlsruhe, GERMANY, F May 30-Jun 01, 2017 [C]. 2017.
[32] JIRSA V K, STACEY W C, QUILICHINI P P, et al. On the nature of seizure dynamics [J]. Brain A Journal of Neurology, 2014, 8): 2210-30.
[33] PROIX T, BARTOLOMEI F, CHAUVEL P, et al. Permittivity Coupling across Brain Regions Determines Seizure Recruitment in Partial Epilepsy [J]. Journal of Neuroscience, 2014.
[34] NICHOLS J M, SEAVER M, TRICKEY S T, et al. Detecting nonlinearity in structural systems using the transfer entropy [J]. Physical Review E Statistical Nonlinear & Soft Matter Physics, 2005, 72(4): 046217.
[35] ASTOLFI L, CINCOTTI F, MATTIA D, et al. Comparison of different multivariate methods for the estimation of cortical connectivity: Simulations and applications to EEG data [J]. Conference proceedings: Annual International Conference of the IEEE Engineering in Medicine and Biology Society IEEE Engineering in Medicine and Biology Society Conference, 2005, 5,4484-7.
[36] FASOULA A, ATTAL Y, SCHWARTZ D. Comparative performance evaluation of data-driven causality measures applied to brain networks [J]. Journal of Neuroscience Methods, 2013, 215(2): 170-89.
[37] SCHREIBER. Measuring information transfer [J]. Physical review letters, 2000, 85(2): 461-4.
[38] SCHROEDER G M, DIEHL B, CHOWDHURY F A, et al. Seizure pathways change on circadian and slower timescales in individual patients with focal epilepsy [J]. Cold Spring Harbor Laboratory, 2019, 20.
[39] MAHARATHI B, WLODARSKI R, BAGLA S, et al. Interictal spike connectivity in human epileptic neocortex [J]. Clinical Neurophysiology, 2018, 130(2).
[40] MA M, WEI X, CHENG Y, et al. Spatiotemporal evolution of epileptic seizure based on mutual information and dynamic brain network [J]. BMC Medical Informatics and Decision Making, 2021, 21(S2).